

Effect of deuteration on phase transitions in $(\text{NH}_4)_3\text{VOF}_5$ © E.V. Bogdanov^{1,2}, V.S. Bondarev^{1,3}, M.V. Gorev^{1,3}, M.S. Molochev^{1,3}, I.N. Flerov^{1,3}¹ Kirensky Institute of Physics, Federal Research Center KSC SB, Russian Academy of Sciences, Krasnoyarsk, Russia² Institute of Engineering Systems and Energy, Krasnoyarsk State Agricultural University, Krasnoyarsk, Russia³ Siberian Federal University, Institute of Engineering Physics and Radio Electronics, Krasnoyarsk, Russia

E-mail: evbogdanov@iph.krasn.ru

Received November 11, 2021

Revised November 11, 2021

Accepted November 13, 2021

The $(\text{ND}_4)_3\text{VOF}_5$ crystal was grown with a high degree of deuteration ($D \approx 92\%$). Structural and thermophysical studies have been carried out, the parameters of phase transitions have been determined. It was found that the deuteration of the ammonium cation in $(\text{NH}_4)_3\text{VOF}_5$ led to a change in the chemical pressure, which was accompanied by an increase in the unit cell volume and an increase in the phase transition temperatures. The baric coefficients dT_i/dp were determined and the phase $T-p$ diagram $(\text{ND}_4)_3\text{VOF}_5$ was constructed. A decrease in the temperature stability of the initial cubic phase $Fm\bar{3}m$ in $(\text{ND}_4)_3\text{VOF}_5$, as well as a wedging out of the intermediate monoclinic phase at a lower pressure as compared to $(\text{NH}_4)_3\text{VOF}_5$, was found.

Keywords: oxyfluorides, phase transitions, heat capacity, thermal expansion, pressure.

DOI: 10.21883/PSS.2022.03.53195.237

1. Introduction

The crystal structure of a number of complex oxyfluorides consists of polar anions $[\text{MO}_x\text{F}_{6-x}]$ [1], the presence of which can lead to the appearance of a macroscopic dipole moment in the bulk crystal and the creation of new polar materials. The closeness of the sizes and electronegativity of oxygen and fluorine ligands leads to disordering of fluorine-oxygen octahedra, and the macroscopic dipole moment in the structure of oxyfluorides as the whole is realized quite rarely [2]. One of the ways to obtain ordered structures of fluorine-oxygen materials is to create an environment of six-coordinated polyhedra, leading to ordering of ligands [3–5]. The procedures for creating ordered oxyfluorides consists in understanding the nature of the disordering of the three-dimensional crystal structure and predicting the possible orientation of local polar moments [6].

Crystals of the vanadium oxyfluoride family are quite diverse, due to the ability of vanadium to change the valence state and form various polar/non-polar fluorine-oxygen anions $[\text{VO}_x\text{F}_{6-x}]$ [7–11]. The presence of two types for bonding of the central atom in octahedra (V–O and V–F) could lead to the possibility of the dipole moment. Complex studies have shown that crystals $(\text{NH}_4)_3\text{VOF}_5$ and $(\text{NH}_4)_3\text{VO}_2\text{F}_4$ have two independent fluorine-oxygen anions in the structure and are characterized by orthorhombic symmetry at room temperature (space group $Immm$) [12,13]. Above room temperature, the crystals undergo transitions to highly symmetrical dynamically disordered phases (space group $Fm\bar{3}m$) with six and twelve space orientations of the fluorine-oxygen octahedra,

respectively, for $(\text{NH}_4)_3\text{VOF}_5$ and $(\text{NH}_4)_3\text{VO}_2\text{F}_4$. Ammonium tetrahedra are disordered and/or partially ordered in the initial cubic and first distorted orthorhombic phases. Upon cooling, the crystals undergo the sequence of phase transformations, accompanied by change in symmetry: $(\text{NH}_4)_3\text{VO}_2\text{F}_4 - Fm\bar{3}m \leftrightarrow Immm(I222) \leftrightarrow \text{ortorhombic} \leftrightarrow P112/m \leftrightarrow P\bar{1}$; $(\text{NH}_4)_3\text{VOF}_5 - Fm\bar{3}m \leftrightarrow Immm \leftrightarrow \leftrightarrow? \leftrightarrow P\bar{1}$ [14,15]. Vibrational spectroscopy data confirm the dynamic character of the structure disorder, and complete freezing of the orientational motion of ammonium groups is observed in $(\text{NH}_4)_3\text{VOF}_5$ and $(\text{NH}_4)_3\text{VO}_2\text{F}_4$ in the area of $T \sim 35$ K [16]. Change in the valence of the central atom ($\text{V}^{4+} \rightarrow \text{V}^{5+}$), accompanied by an increase in its ionic radius ($C_N = 6 - R_{\text{V}^{4+}} = 0.58$ Å; $R_{\text{V}^{5+}} = 0.54$ Å), leads to the decrease in chemical pressure in $(\text{NH}_4)_3\text{VOF}_5$ and an increase ($\sim 1.5\%$) of the unit cell volume compared to $(\text{NH}_4)_3\text{VO}_2\text{F}_4$, as well as to the number of features in the behavior of physical properties. In particular, there is a significant change, firstly, in the temperatures of phase transitions, secondly, sensitivity of the initial and distorted phases to hydrostatic pressure, and thirdly, total entropy of phase transformations [14,15]. The latter fact agrees with the disordering model of structural elements in the initial cubic phase $Fm\bar{3}m$ [13]. At the same time, the nature of structural distortions remains ferroelastic (non-ferroelectric).

The possibility of changing the degree of disorder of fluorine-oxygen anions is shown by the example of the substitution of the $A, A' = \text{NH}_4, \text{ND}_4, \text{K}, \text{Cs}, \text{Rb}$ cation in inter-octahedral cavity of compounds $AA'\text{MO}_2\text{F}_4$ [17,18]. Deuteration of the ammonium group in $(\text{NH}_4)_3\text{VO}_2\text{F}_4$ led to a decrease in the chemical pressure, while the volume

unit cell increased ($\sim 1.5\%$) to $(\text{ND}_4)_3\text{VO}_2\text{F}_4$ compared to $(\text{NH}_4)_3\text{VO}_2\text{F}_4$ [19]. As a result of deuteration, the second orthorhombic phase in $(\text{ND}_4)_3\text{VO}_2\text{F}_4$ is wedged out and instead of a sequence of phase transitions $Immm \leftrightarrow \text{orthorhombic phase} \leftrightarrow P112/m$ there is a direct transition $Immm \leftrightarrow P112/m$. [14]. The deuteration also led to a decrease in the individual phase transition entropies $Fm\bar{3}m \leftrightarrow Immm$ and $Immm \leftrightarrow P112/m$. The value of total entropy change $\Sigma\Delta S_i \approx R \cdot \ln 6$ in $(\text{ND}_4)_3\text{VO}_2\text{F}_4$, associated with the distortion of the structure as the symmetry of the crystal lattice decreases from cubic to triclinic, turned out to be much smaller than in the protonated compound. The decrease in the total entropy $\Sigma\Delta S_i$ as a result of deuteration indicates the significant role of the anharmonicity degree of vibrations of ammonium tetrahedra.

In this work, we study the effect of deuteration on the thermodynamic properties of vanadium oxopenafluoride $(\text{NH}_4)_3\text{VOF}_5$ in the area of phase transitions resulting from disordering/ordering of structure elements.

2. Experimental methods and research results

To obtain the deuterated compound, the initial crystal $(\text{NH}_4)_3\text{VOF}_5$ was dissolved in heavy water ($\sim 99.9\% \text{D}$). Next, the solution was placed in a desiccator with P_2O_5 and kept there until complete absorption of water. The process of recrystallization in heavy water was repeated several times to achieve the maximum degree of deuteration. The percent of deuterium $\text{D} \approx 92\%$ was determined by comparing the intensities of the NMR absorption lines ^1H of the protonic and deuterated compounds [20].

Powder X-ray pattern $(\text{ND}_4)_3\text{VOF}_5$ is obtained at room temperature on the D8 ADVANCE diffractometer by Bruker using the VANTEC linear detector and $\text{Cu-K}\alpha$ radiation (Fig. 1, *a*). The detector step was equal to 0.016° , the exposure at each point was 0.6 s. The main reflections on the X-ray pattern were indexed in a orthorhombic structure (space group $Immm$), with parameters close to $(\text{NH}_4)_3\text{VO}_2\text{F}_4$ [12]. Therefore, the structure of this oxyfluoride was used as the initial model for refinement. The only one change was related to the correction of the occupancies of the positions of the fluorine and oxygen atoms in order to make the final formula correspond to $(\text{ND}_4)_3\text{VOF}_5$. As a result, the initially completely ordered polyhedra VO_2F_4 had to be disordered over 2 positions in order to obtain the polyhedra VOF_5 , since through VO_2F_4 passed through the plane of symmetry m , which did not allow ordering the group VOF_5 (Fig. 1, *b*). The X-ray pattern also revealed several weak peaks that do not belong to the phase $(\text{ND}_4)_3\text{VOF}_5$. Some of them were associated with the phase $(\text{NH}_4)_2\text{VOF}_4$, which turned out to be $\sim 13\%$ by weight. The refinement by the Rietveld method was carried out in the TOPAS 4.2 program [21] and gave low values of the R factors (Table 1, Fig. 1, *a*).

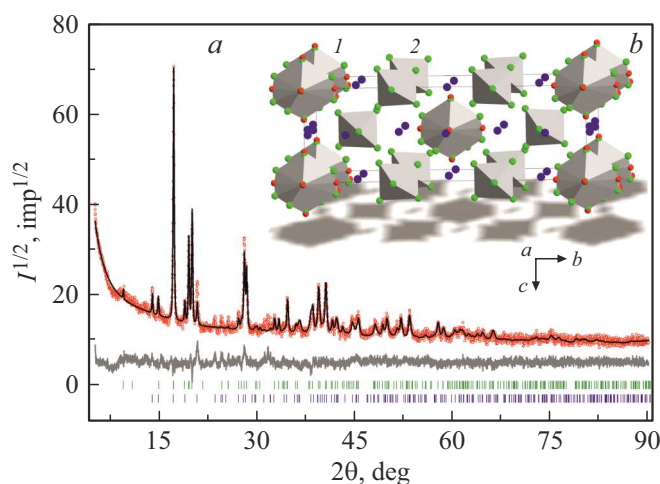


Figure 1. Results of refinement of the structure $(\text{ND}_4)_3\text{OF}_5$ by the Rietveld method (*a*). The crystal structure (*b*) (1 — VOF_5 is disordered over many positions, 2 — VOF_5 is disordered over two positions).

As a result of studying the temperature dependence of thermal expansion, information was obtained on the presence and temperatures of phase transformations in $(\text{ND}_4)_3\text{VOF}_5$. The measurements were carried out on a NETZSCH induction dilatometer DIL-402C in the temperature range of 120–420 K in dynamic mode with a heating rate of $\sim 3 \text{ K/min}$, in a gaseous helium flow at a flow rate of $\sim 50 \text{ ml/min}$. Fused quartz standards were used to calibrate the device and take into account the thermal expansion of the measuring system [22]. The samples under study were prepared from powder $(\text{ND}_4)_3\text{VOF}_5$ in the form of tablets with diameter of $\sim 4 \text{ mm}$ and the height of $\sim 4\text{--}6 \text{ mm}$ by pressing at a pressure of $\sim 2 \text{ GPa}$.

The temperature behavior of the deformation and the volume expansion coefficient $(\text{ND}_4)_3\text{VOF}_5$ (Fig. 2) are in qualitative agreement with the dependences $\Delta V/V_0(T)$ and $\beta(T)$ obtained earlier for $(\text{NH}_4)_3\text{VOF}_5$ [15]. Additional anomalies caused by the presence of small amount of impurities were not found. A number of differences are associated with the magnitude of the change in deformation

Table 1. Main parameters for crystal structure refinement $(\text{ND}_4)_3\text{VOF}_5$

Sp. gr.	<i>Immm</i>
<i>a</i> , Å	9.1553 (10)
<i>b</i> , Å	18.929 (4)
<i>c</i> , Å	6.3072 (13)
<i>V</i> , Å ³	1093.1 (3)
2θ interval, °	5–90
R_{wp} , %	10.17
R_{p} , %	7.83
R_{B} , %	4.85
χ^2	2.09

and the temperatures of phase transitions. Anomalous deformation behavior in $(\text{ND}_4)_3\text{VOF}_5$ at $T_1 = 355 \pm 1$ K associated with the first-order transition is accompanied by significant jump $\delta(V/V_0)(T_1) = 2 \cdot 10^{-2}$ (Fig. 2, *b*). In the low-temperature region, the sequence of two weakly pronounced anomalies is observed, which are more clearly manifested in the temperature dependence of the volumetric thermal expansion coefficient: $\Delta\beta(T_2) = 0.25 \cdot 10^{-4}$ 1/K and $\Delta\beta(T_3) = 0.65 \cdot 10^{-4}$ 1/K (Fig. 2, *a*).

Studies of the temperature dependence of the heat capacity of $C_p(T)$ $(\text{ND}_4)_3\text{VOF}_5$ using the adiabatic calorimetry method made it possible to refine the phase transition temperatures and determine their energy and entropy characteristics. The powder sample with total mass of ~ 0.3 g was hermetically packed in the inert helium atmosphere in furniture with the heater. The heat capacity of the system was measured in continuous ($dT/dt = 0.15$ K/min)

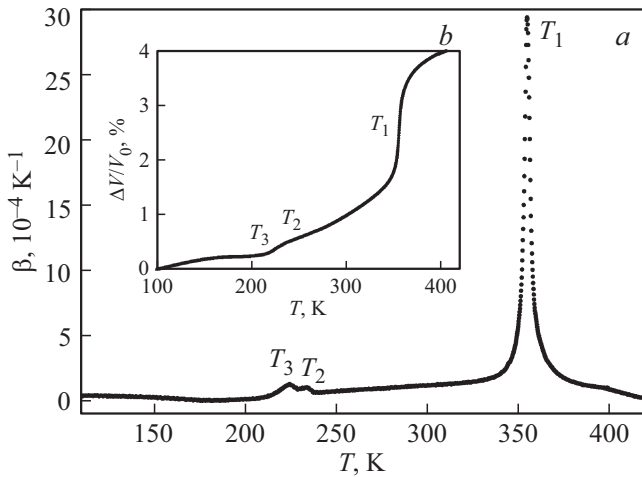


Figure 2. Temperature dependences of volume expansion coefficient (*a*) and deformation (*b*) $(\text{ND}_4)_3\text{VOF}_5$.

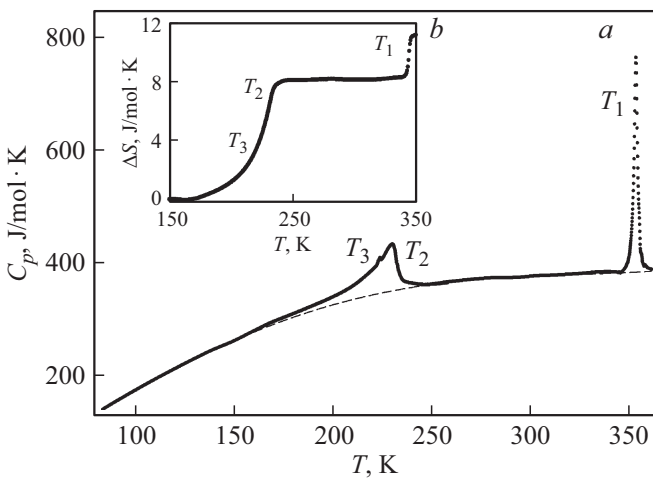


Figure 3. Temperature dependences of the heat capacity (*a*) and entropy of phase transitions (*b*) in $(\text{ND}_4)_3\text{VOF}_5$ over the wide temperature range. Dashed line — lattice heat capacity.

Table 2. Thermodynamic parameters of phase transitions in oxyfluorides $(\text{NH}_4)_3\text{VOF}_5$ and $(\text{ND}_4)_3\text{VOF}_5$

Parameter	$(\text{NH}_4)_3\text{VOF}_5$ [15]	$(\text{ND}_4)_3\text{VOF}_5$
T_1 , K	348.1 ± 0.5	353.2 ± 0.5
ΔS_1 , J/mol · K	5.4 ± 0.5	3.0 ± 0.3
$(dT_1/dp)_{\text{calc}}$, K/GPa	115	93
T_2 , K	229.1 ± 0.2	230.2 ± 0.2
$(A_T^2/B)_{T_2}$, J/mol · K ²	-0.6	-0.5
$(A_T^3/C)_{T_2}$, J ² /mol ² · K ³	4.6	6.3
$T_2 - T_{C2}$, K	3.2	6.3
N_2	-0.13	-0.19
ΔS_2 , J/mol · K	7.6 ± 0.7	7.9 ± 0.7
$(dT_2/dp)_{\text{exp}}$, K/GPa	23 ± 2	—
$(dT_2/dp)_{\text{calc}}$, K/GPa	26	13
T_3 , K	218 ± 1	224 ± 1
$(A_T^2/B)_{T_3}$, J/mol · K ²	—	-0.29
$(A_T^3/C)_{T_3}$, J ² /mol ² · K ³	—	2.1
$T_3 - T_{C3}$, K	—	6.1
N_3	—	-0.19
ΔS_3 , J/mol · K	0.4 ± 0.06	0.2 ± 0.05
$(dT_3/dp)_{\text{exp}}$, K/GPa	92 ± 4	—
$(dT_3/dp)_{\text{calc}}$, K/GPa	120	88

and discrete ($\Delta T = 2.5$ – 3.0 K) heating modes. The heat capacity of the furniture was measured in the separate experiment.

The temperature behavior of the molar isobaric heat capacity $(\text{NH}_4)_3\text{VOF}_5$ (Fig. 3, *a*) is qualitatively agrees with the $C_p(T)$ dependence obtained for the protonated compound [15]. Comparison of refined temperatures of phase transitions occurring in $(\text{NH}_4)_3\text{VOF}_5$ and $(\text{ND}_4)_3\text{VOF}_5$ shows that deuteration led to their growth (Table 2).

3. Discussion of results

The high degree of deuteration of vanadium oxopentafluoride $(\text{NH}_4)_3\text{VOF}_5$ ($\sim 92\%$ D) did not change the symmetry of the realized at room temperature orthorhombic phase (space group *Immm*). At the same time, the unit cell volume is $(\text{ND}_4)_3\text{VOF}_5$ compared to protonated vanadate $(\text{NH}_4)_3\text{VOF}_5$ increased by only $\sim 0.2\%$. The obtained value differs significantly from the value of the change in the volume of the unit cell, which accompanied the deuteration of vanadium dioxotetrafluoride $(\text{NH}_4)_3\text{VO}_2\text{F}_4$ ($\sim 1.5\%$) [19]. The small change in volume upon deuteration of the ammonium cation was observed in the oxyfluoride system $(\text{NH}_4)_2\text{MO}_2\text{F}_4$ ($M = \text{Mo}, \text{W}$) with isolated octahedra [20,23]. Estimation of the change in chemical pressure $\Delta p \approx \Delta T/(dT/dp)$ in $(\text{ND}_4)_3\text{VOF}_5$ was performed using the phase T – p diagram of the initial crystal $(\text{NH}_4)_3\text{VOF}_5$ and changes in phase transformation temperatures as the result of substitution $\text{D} \rightarrow \text{H}$. The obtained value $\Delta p \approx 0.1$ GPa turned out to be quite close to the value ($\Delta p \approx -0.08$ GPa) obtained earlier when studying the effect of deuteration $(\text{NH}_4)_3\text{VO}_2\text{F}_4$. Thus, ammonium

vanadium oxyfluorides, whose structure consists of linked $[\text{VO}_x\text{F}_{6-x}]$ octahedra, are characterized by the much greater sensitivity to changes in chemical pressure resulting from the substitution of $\text{D} \rightarrow \text{H}$ than ammonium oxyfluorides $(\text{NH}_4)_2\text{WO}_2\text{F}_4$ and $(\text{NH}_4)_2\text{MoO}_2\text{F}_4$ with isolated octahedra ($\Delta p \approx 0.02$ GPa) [20,23].

To determine the energy and entropy characteristics of phase transitions in $(\text{ND}_4)_3\text{VOF}_5$, the heat capacity is separated into the regular C_{reg} and the anomalous $\Delta C_p(T)$ associated with the transition sequence, contributions. To this end, the sections of the temperature dependence of the heat capacity outside the area of existence of anomalies were considered as corresponding to C_{reg} and were approximated by combination of the Debye and Einstein functions. Interpolation of the function $C_{\text{reg}}(T)$ on the areas of anomalous behavior $C_p(T)$ made it possible to determine the excess heat capacity (Figs. 3, *a* and 4, *a*). The values of the entropy change $\Delta S_i = \int (\Delta C_p/T) dT$ obtained by integrating the temperature dependence of $\Delta C_p(T)$ are presented in Table 2.

The deuteration of $(\text{NH}_4)_3\text{VOF}_5$ led to significant decrease in the entropy of the high-temperature phase transformation ΔS_1 (Table 2), which indirectly confirms its connection with the ordering processes of both fluorine-oxygen octahedra and ammonium tetrahedra [15]. The anomalous behavior of thermophysical properties in the low-temperature region, which is characteristic of second-order phase transitions, has not changed. This fact made it possible to analyze the temperature dependence of the excess heat capacity $\Delta C_p(T)$ in the framework of Landau's thermodynamic theory [24] (Fig. 4, *a*) and determine the entropy change ΔS_2 and ΔS_3 , as well as the number of other phase transition parameters for T_2 and T_3 . The square of the inverse excess heat capacity near low-temperature phase transitions in $(\text{ND}_4)_3\text{VOF}_5$ is fairly well described by linear temperature function (Fig. 4, *b*): $(\Delta C_p/T)^{-2} = [2 \cdot (B^2 - 3 \cdot A^2 C)^{0.5} / A_T^2]^2 + 12 \cdot C(T_0 - T) / A_T^3$, where the values are $A = A_T \cdot (T_0 - T_C) + A_T \cdot (T - T_0) = A' + A_T \cdot (T - T_0)$, B and C are thermodynamic potential coefficients: $\Delta \Phi(p, T, \eta) = A \cdot \eta^2 + B \cdot \eta^4 + C \cdot \eta^6$ (η — transition parameter, T_C — Curie temperature, T_0 — phase transition temperature).

It turned out that the entropies of low-temperature phase transformations did not practically change as a result of $\text{D} \rightarrow \text{H}$ substitution (Table 2), which, in turn, confirms the preferred contribution of fluorine-oxygen octahedra to the mechanism of phase transitions of the ordering and displacement types, respectively, at T_2 and T_3 .

Comparison of the phenomenological parameters of vanadium oxyfluorides showed (Table 2) that, as the result of deuteration, low-temperature transformations into $(\text{ND}_4)_3\text{VOF}_5$ turned out to be significantly farther from the tricritical point ($T_i - T_{Ci} = 0$ and $N = 0$, where $N = \pm [B^2 / (3 \cdot A_T C T_0)]^{-0.5}$ is the degree of closeness of the transition to the tricritical point than the corresponding phase transitions in $(\text{NH}_4)_3\text{VOF}_5$ [15].

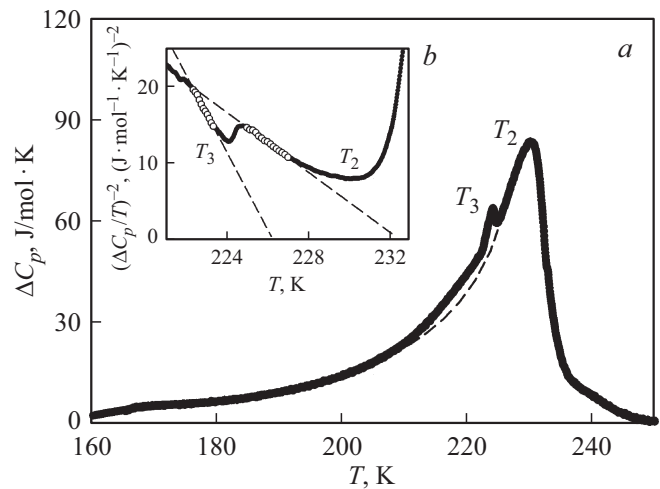


Figure 4. Temperature dependences of the excess heat capacity (*a*) and the square of its reciprocal (*b*) in the vicinity of T_2 and T_3 .

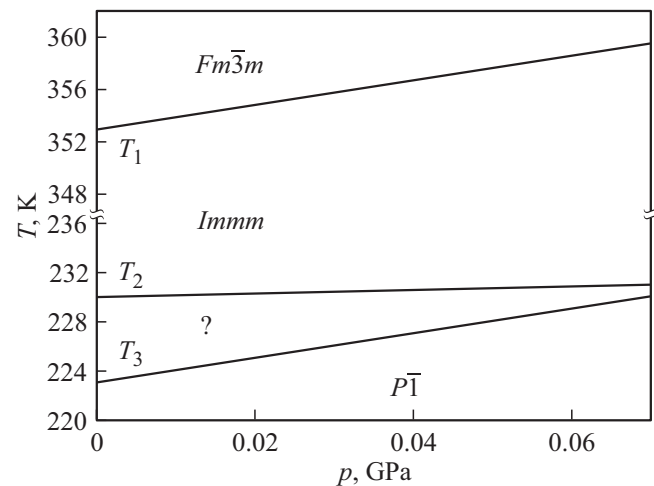


Figure 5. Temperature-pressure phase diagram of the crystal $(\text{ND}_4)_3\text{VOF}_5$, constructed based on the calculation of pressure coefficients $(dT_i/dp)_{\text{calc}}$.

Joint analysis of the experimental calorimetric and dilatometric data made it possible to estimate the pressure coefficients dT_i/dp in $(\text{ND}_4)_3\text{VOF}_5$ (Table 2). The value of dT_1/dp for the high-temperature transformation is calculated from the Clapeyron–Clausius equation for first-order transitions, and the coefficients dT_2/dp and dT_3/dp for phase transitions of the second order are defined in line with the Ehrenfest formula ($\Delta C_p = \Delta \beta \cdot T_i / (dT_i/dp)_p = 0$) [25].

Similar estimates of pressure coefficients made earlier for $(\text{NH}_4)_3\text{VOF}_5$ [15] showed good agreement between the calculated quantities dT_i/dp and obtained by direct measurements.

Based on data on phase transition temperatures and calculated pressure coefficients, the phase T – p diagram $(\text{ND}_4)_3\text{VOF}_5$ (Fig. 5), which qualitatively corresponds to

the diagram of the protonated crystal $(\text{NH}_4)_3\text{VOF}_5$, is constructed. Thus, we can conclude that the deuteration of the ammonium cation did not change the phase symmetry and the sequence of ferroelastic phase transitions $Fm\bar{3}m \leftrightarrow Immm \leftrightarrow monoclinic \leftrightarrow P\bar{1}(P1)$.

Deuteration of $(\text{NH}_4)_3\text{VOF}_5$ leads to an increase in the temperature T_1 of the high-temperature phase transition in $(\text{ND}_4)_3\text{VOF}_5$, which is accompanied by decrease in the pressure coefficient dT_1/dp . As a result, on the phase $T-p$ diagram $(\text{ND}_4)_3\text{VOF}_5$, the area of existence of the initial cubic phase (space group $Fm\bar{3}m$) narrows, and the orthorhombic phase (space group $Immm$) becomes energetically favorable in a wider temperature range. The substitution $D \rightarrow H$ affects both the temperatures T_2 and T_3 and the pressure coefficients dT_2/dp and dT_3/dp . As a result, on the phase $T-p$ diagram $(\text{ND}_4)_3\text{VOF}_5$ takes place the narrowing the stability area of the intermediate *monoclinic* phase and subsequent wedging-out with increasing external pressure. The triple-point in $(\text{ND}_4)_3\text{VOF}_5$ is realized at a lower overpressure $p_{tr} \approx 0.08$ GPa ($p_{tr} \approx 0.1$ GPa in the case of $(\text{NH}_4)_3\text{VOF}_5$ [15]). The change in the area of stability of the high-temperature cubic phase and the shift of the triple-point in $(\text{ND}_4)_3\text{VOF}_5$ at low pressures is consistent with the behavior of phase transitions in $(\text{NH}_4)_3\text{VOF}_5$ with increasing external hydrostatic pressure.

Complex studies of deuterated crystals $(\text{ND}_4)_3\text{VOF}_5$ and $(\text{ND}_4)_3\text{VO}_2\text{F}_4$ [15] showed that substitution $D \rightarrow H$ leads not only to change in phase transition temperatures, but also to the significant change in the structural, energy and baric characteristics of phase transitions resulting from changes in chemical pressure. On the other hand, the chemical pressure associated with the deuteration of the ammonium cation does not change the nature and mechanisms of phase transformations.

Ferroelastic phase transitions occurring in vanadium oxyfluorides are accompanied by significant changes in entropy $\Sigma\Delta S_i$ and pressure coefficients dT_i/dp . Therefore, the compounds $(\text{NH}_4)_3\text{VOF}_5$ and $(\text{NH}_4)_3\text{VO}_2\text{F}_4$ may be of interest from the point of view of studying their barocaloric efficiency.

4. Conclusion

Crystals of deuterated vanadium (IV) oxopentafluoride, $(\text{ND}_4)_3\text{VOF}_5$, have been grown, and thermophysical properties have been studied in a wide temperature range.

1. It has been found that substitutions $D \rightarrow H$ did not affect the sequence of ferroelastic phase transitions in $(\text{ND}_4)_3\text{VOF}_5$.

2. Deuteration led to a change in the chemical pressure, which is accompanied by an increase in the volume of the unit cell and an increase in the phase transition temperatures in $(\text{ND}_4)_3\text{VOF}_5$.

3. The pressure coefficients dT_i/dp are estimated and the proposed $T-p$ phase diagram is constructed.

4. The value of the excess chemical pressure in $(\text{ND}_4)_3\text{VOF}_5$ is determined based on the analysis of the phase $T-p$ diagram $(\text{NH}_4)_3\text{VOF}_5$ and turned out to be close to the value of the pressure change that occurs during deuteration $(\text{NH}_4)_3\text{VOF}_5$.

5. Decrease in the temperature stability of the initial cubic phase in $(\text{ND}_4)_3\text{VOF}_5$, as well as wedging out of the intermediate *monoclinic* phase at a lower pressure compared with $(\text{NH}_4)_3\text{VOF}_5$.

6. Deuteration of $(\text{NH}_4)_3\text{VOF}_5$ leads to the decrease in ΔS_1 , which indirectly confirms the connection between the phase transition at T_1 and ordering of the fluorine-oxygen octahedra and ammonium tetrahedra.

7. It is shown that low-temperature transformations into $(\text{ND}_4)_3\text{VOF}_5$ as the result of deuteration are characterized by lower degree of proximity to the tricritical point than the corresponding transitions in $(\text{NH}_4)_3\text{VOF}_5$.

8. Decrease in total entropy change $\Sigma\Delta S_i \approx R \cdot \ln 4$ to $(\text{ND}_4)_3\text{VOF}_5$ versus $\Sigma\Delta S_i \approx R \cdot \ln 6$ in $(\text{NH}_4)_3\text{VOF}_5$ indicates the participation of the ammonium cation in the processes of structure ordering, as well as the possibility of the anharmonicity degree of vibrations reducing of ammonium tetrahedra as a result of deuteration.

Acknowledgments

X-ray and dilatometric data were obtained using the equipment of the Krasnoyarsk Regional Center for Collective Use of the Federal Research Center — Krasnoyarsk Science Center of the Siberian Branch of the Russian Academy of Sciences.

Conflict of interest

The authors declare that they have no conflict of interest.

References

- [1] G. Pausewang, K. Dehnicke. *Z. Anorg. Allg. Chem.* **369**, 265 (1969).
- [2] N.F. Stephens, M. Buck, P. Lightfoot. *J. Mater. Chem.* **15**, 4298 (2005).
- [3] F.H. Aidoudi, C. Black, K.S. Athukorala Arachchige, A.M.Z. Slawin, R.E. Morris, P. Lightfoot. *Dalton Trans.* **43**, 568 (2014).
- [4] R. Gautier, M.D. Donakowski, K.R. Poepelmeier. *J. Solid State Chem.* **195**, 132 (2012).
- [5] G.A. Senchyk, V.O. Bukhan'ko, A.B. Lysenko, H. Krautscheid, B. Rusanov, A.N. Chernega, M. Karbowski, K.V. Domasevitch. *Inorg. Chem.* **51**, 8025 (2012).
- [6] R.A.F. Pinlac, M.R. Marvel, J.J.-M. Lesage, K.R. Poepelmeier. *Mater. Res. Soc. Symp. Proc.* **1148**, PP01-04 (2009).
- [7] R.L. Davidovich, L.G. Kharlamova, L.V. Samarets. *Coordination chemistry* **3**, 850 (1977).
- [8] B.R. Wani, U.R.K. Rao, K.S. Venkateswarlu, A.S. Gokhale. *Thermochim. Acta* **58**, 87 (1982).
- [9] K. Kobayashi, T. Matsuo, H. Suga, S. Khairoun, A. Tressaud. *Solid State Commun.* **53**, 719 (1985).

- [10] P. Bukovec, N. Bukovec, A. Demšar. *J. Therm. Anal.* **36**, 1751 (1990).
- [11] B. Dojer, M. Kristl, Z. Jagličić, M. Drogenik, A. Meden. *Acta Chim. Slov.* **55**, 834 (2008).
- [11] S.J. Patwe, S.N. Achary, K.G. Girija, C.G.S. Pillai, A.K. Tyagi. *J. Mater. Res.* **25**, 1251 (2010).
- [12] M. Leimkühler, R.J. Mattes. *Solid State Chem.* **65**, 260 (1986).
- [13] A.A. Udovenko, E.I. Pogoreltsev, Y.V. Marchenko, N.M. Laptash. *Acta Cryst. B* **73**, 1 (2017).
- [14] V.D. Fokina, M.V. Gorev, A.G. Kocharova, E.I. Pogoreltsev, I.N. Flerov. *Solid State Sci.* **11**, 836 (2009).
- [15] E.V. Bogdanov, E.I. Pogoreltsev, A.V. Kartashev, M.V. Gorev, M.S. Molokeev, S.V. Melnikova, I.N. Flerov, N.M. Laptash. *Physics of the Solid State* **62**, 7, 1123 (2020).
- [16] Yu.V. Gerasimova, A.S. Oreshonkov, N.M. Laptash, A.N. Vtyurin, A.S. Krylov, N.P. Shestakov, A.A. Ershov, A.G. Kocharova. *Spectrochim. Acta A* **176**, 106 (2017).
- [17] E.V. Bogdanov, A.D. Vasil'ev, I.N. Flerov, N.M. Laptash. *Physics of the Solid State* **53**, 2, 284 (2011).
- [18] E.V. Bogdanov, E.I. Pogoreltsev, M.V. Gorev, I.N. Flerov. *Inorg. Chem.* **56**, 11, 6706 (2017).
- [19] E.V. Bogdanov, E.I. Pogoreltsev, M.V. Gorev, M.S. Molokeev, I.N. Flerov. *Physics of the Solid State* **61**, 2, 330 (2019).
- [20] E.V. Bogdanov, S.V. Mel'nikova, E.I. Pogoreltsev, M.S. Molokeev, I.N. Flerov. *Solid State Sci.* **61**, 155 (2016).
- [21] Bruker AXS TOPAS V4: General profile and structure analysis software for powder diffraction data. User's Manual. Bruker AXS, Karlsruhe, Germany. (2008).
- [22] M.V. Gorev, E.V. Bogdanov, I.N. Flerov, A.G. Kocharova, N.M. Laptash. *Physics of the Solid State* **52**, 1, 156 (2010).
- [23] I.N. Flerov, V.D. Fokina, M.V. Gorev, E.V. Bogdanov, M.S. Molokeev, A.F. Bovina, A.G. Kocharova. *Physics of the Solid State* **49**, 6, 1093 (2007).
- [24] K.S. Aleksandrov, I.N. Flerov. *Physics of the Solid State* **21**, 327 (1979).
- [25] N. Parsonage, L. Staveley. *Disorder in Crystals (Besporjadok v kristallakh)*. Mir, M. (1982) 436 p.(in Russian).

Editor Yu.E. Kitayev